Calcineurin promotes adaptation to chronic stress through two distinct mechanisms

Mackenzie J. Flynn[a,b], Nicholas W. Harper[b,c], Rui Li[a], Lihua Julie Zhu[a,d,e], Michael J. Lee[c], and Jennifer A. Benanti[a,*]

[a]Department of Molecular, Cell and Cancer Biology, University of Massachusetts Chan Medical School, Worcester, MA 01605; [b]Interdisciplinary Graduate Program, Morningside Graduate School of Biomedical Sciences, University of Massachusetts Chan Medical School, Worcester, MA 01605; [c]Department of Systems Biology, University of Massachusetts Chan Medical School, Worcester, MA 01605; [d]Department of Genomics and Computational Biology, University of Massachusetts Chan Medical School, Worcester, MA 01605; [e]Program in Molecular Medicine, University of Massachusetts Chan Medical School, Worcester, MA 01605

ABSTRACT **Adaptation to environmental stress requires coordination between stress-defense programs and cell cycle progression. The immediate response to many stressors has been well characterized, but how cells survive in challenging environments long term is unknown. Here, we investigate the role of the stress-activated phosphatase calcineurin (CN) in adaptation to chronic $CaCl_2$ stress in *Saccharomyces cerevisiae*. We find that prolonged exposure to $CaCl_2$ impairs mitochondrial function and demonstrate that cells respond to this stressor using two CN-dependent mechanisms—one that requires the downstream transcription factor Crz1 and another that is Crz1 independent. Our data indicate that CN maintains cellular fitness by promoting cell cycle progression and preventing $CaCl_2$-induced cell death. When Crz1 is present, transient CN activation suppresses cell death and promotes adaptation despite high levels of mitochondrial loss. However, in the absence of Crz1, prolonged activation of CN prevents mitochondrial loss and further cell death by upregulating glutathione biosynthesis genes thereby mitigating damage from reactive oxygen species. These findings illustrate how cells maintain long-term fitness during chronic stress and suggest that CN promotes adaptation in challenging environments by multiple mechanisms.**

SIGNIFICANCE STATEMENT

- The immediate response to environmental stress is well-defined, but how cells survive in challenging environments long-term is unknown.
- The response to chronic $CaCl_2$ stress was investigated in budding yeast and found to be distinct from the immediate stress response. The phosphatase calcineurin coordinates this adaptive response by two mechanisms that differentially require the downstream transcription factor Crz1.
- These findings reveal functions of calcineurin in promoting adaptation during prolonged stress exposure and provide a framework for future studies investigating the long-term response to additional environmental stressors.

Monitoring Editor
Doug Kellogg
University of California, Santa Cruz

Received: Mar 20, 2024
Revised: Jul 15, 2024
Accepted: Jul 24, 2024

New Hypothesis

INTRODUCTION

Cells must balance the conflicting demands of proliferation and stress-defense to survive in a constantly changing environment. Under optimal growth conditions, cellular energy is predominately used to support growth and division (López-Maury *et al.*, 2008; Ho and Gasch, 2015). While prioritizing proliferation ensures competitive fitness in standard conditions, rapid growth results in a reduced ability to respond to stress, which decreases fitness in suboptimal environments. Thus, in response to environmental changes, cells distribute cellular resources between growth-related processes and those providing tolerance to stress.

Slow growing cells are more resistant to stress and exhibit increased survival in challenging environments (Elliott and Futcher, 1993; Lu *et al.*, 2008; Zakrzewska *et al.*, 2011). Cells often induce a transient cell cycle arrest in response to stress, which provides protection against subsequent stress exposure (Bonny *et al.*, 2021). While cell division is paused, cells redistribute intracellular resources to orchestrate changes in transcription, translation, and posttranslational modifications (López-Maury *et al.*, 2008; Ho and Gasch, 2015). In yeast, the immediate response to many stressors includes the induction of a transcriptional program called the environmental stress response (ESR) (Gasch *et al.*, 2000; Causton *et al.*, 2001). Approximately 300 genes required for stress-tolerance are induced by the ESR, including genes related to detoxification, cell wall integrity, and DNA damage repair. Nearly 600 genes involved in growth-related processes such as ribosome biogenesis, RNA metabolism, and nucleotide biosynthesis are also repressed by the ESR. In addition to the ESR, which provides general protection in diverse environments, most stressors also require stress-specific changes in transcription, translation, and posttranslational modifications. As cells adapt, many of these gene expression changes are reversed and cells resume cycling. Importantly, while the immediate response to stress is well characterized, very little is known about the physiological changes that occur after cells recover from a transient stress-induced cell cycle arrest and shut off the ESR transcriptional program.

The Ca^{2+}/calmodulin-activated phosphatase calcineurin (CN) is a conserved stress-response regulator. In humans, CN is best characterized for its regulation of NFAT family transcription factors during the immune response and CN inhibitors are widely used as immunosuppressive drugs (Hogan *et al.*, 2003; Vaeth and Feske, 2018). Mammalian CN is also activated in response to environmental stressors such as nutrient deprivation and oxidative stress, which trigger the release of lysosomal Ca^{2+} (Medina *et al.*, 2015; Zhang *et al.*, 2016). In response to these signals, CN dephosphorylates and activates the transcription factor TFEB to promote the expression of lysosome biogenesis and autophagy genes.

In yeast, CN is comprised of a catalytic (CNA) subunit and a regulatory (CNB) subunit and is activated when Ca^{2+}/calmodulin binds to CNA and disrupts an autoinhibitory interaction (Cyert, 2003; Roy and Cyert, 2019). CN deficiency can be accomplished by deletion of the CNA or CNB subunits or by treating cells with CN inhibitors (FK506 or cyclosporin A) (Liu, 1993; Cyert, 2003). As in human cells, CN is similarly activated by the increase in cytosolic Ca^{2+} that occurs in response to many environmental stressors including cell wall damage, alkaline pH, osmotic imbalance, and toxic cations (Cyert, 2003; Cyert and Philpott, 2013). Upon activation, CN dephosphorylates target substrates involved in various cellular processes including protein trafficking, membrane structure/function, transcription, translation, cell cycle, ubiquitin signaling, and polarized growth (Goldman *et al.*, 2014).

The transcription factor Crz1 is the best characterized target of CN and is thought to be the major effector of the CN-dependent stress response (Stathopoulos and Cyert, 1997). Following dephosphorylation by CN, Crz1 translocates to the nucleus and induces the expression of approximately 160 target genes with broad functions in adaptation including ion homeostasis, vesicular transport, and cell wall maintenance (Yoshimoto *et al.*, 2002). Crz1 target genes also include negative regulators of CN signaling which shut off CN activity once cells have adapted. In addition to regulating the expression of genes important for adaptation, CN delays cell cycle progression in collaboration with the MAPKs Hog1 and Mpk1 (Mizunuma *et al.*, 1998, 2001; Yokoyama *et al.*, 2006; Leech *et al.*, 2020; Flynn and Benanti, 2022).

Many CN-dependent functions have been characterized in response to $CaCl_2$ since CN is strongly activated by this stressor. However, inactivation of CN has been reported to have no effect on proliferation in the presence of moderate levels of $CaCl_2$, and to confer resistance at very high concentrations (Nakamura *et al.*, 1996; Matheos *et al.*, 1997; Withee *et al.*, 1997, 1998; Mulet *et al.*, 2006; Ferreira *et al.*, 2012; Xu *et al.*, 2019). In contrast, Crz1 has been shown to promote proliferation in response to $CaCl_2$, though reported phenotypes differ in severity (Polizotto and Cyert, 2001; Mulet *et al.*, 2006; Ferreira *et al.*, 2012; Zhao *et al.*, 2013; Xu *et al.*, 2019). Given these observations, it is unclear whether CN signaling is important for survival during $CaCl_2$ stress.

Here, we characterized the physiological response of *Saccharomyces cerevisiae* to long-term growth in $CaCl_2$ and investigated the impact of CN and Crz1 on cellular fitness in this environment. We show that chronic $CaCl_2$ exposure triggers a decrease in proliferation rate as well as the loss of functional mitochondria. Using coculture competitive fitness assays, we determined that CN is required for fitness during prolonged $CaCl_2$ exposure and maintains fitness by both Crz1-dependent and Crz1-independent mechanisms. Our findings demonstrate how cells adapt to prolonged $CaCl_2$ exposure and suggest that CN promotes cellular fitness by multiple mechanisms.

RESULTS

CN promotes fitness in response to chronic calcium stress

We set out to determine the importance of CN signaling for survival in $CaCl_2$ stress. Consistent with previous studies, deletion of the CN-regulatory subunit *CNB1* had no detectable effect on the proliferation of cells growing on agar plates containing 0.2 M $CaCl_2$ (Figure 1A) (Nakamura *et al.*, 1996; Withee *et al.*, 1997, 1998; Mulet *et al.*, 2006; Ferreira *et al.*, 2012; Xu *et al.*, 2019). Because growth

This article was published online ahead of print in MBoC in Press (http://www.molbiolcell.org/cgi/doi/10.1091/mbc.E24-03-0122) on July 31, 2024.

Author contributions: M.J.F., N.W.H., M.J.L., and J.A.B. conceived and designed the experiments; M.J.F. and N.W.H. performed the experiments; M.J.F., N.W.H., R.L., L.J.Z., M.J.L., and J.A.B. analyzed the data; M.J.F. and J.A.B. drafted the article; M.J.F. prepared the digital images.

*Address correspondence to: Jennifer A. Benanti (jennifer.benanti@umassmed.edu).

Abbreviations used: CHX, cycloheximide; CN, calcineurin; ESR, environmental stress response; ETC, electron transport chain; GSH, glutathione; MAPK, mitogen-activated protein kinase; PI, propidium iodide; ROS, reactive oxygen species.

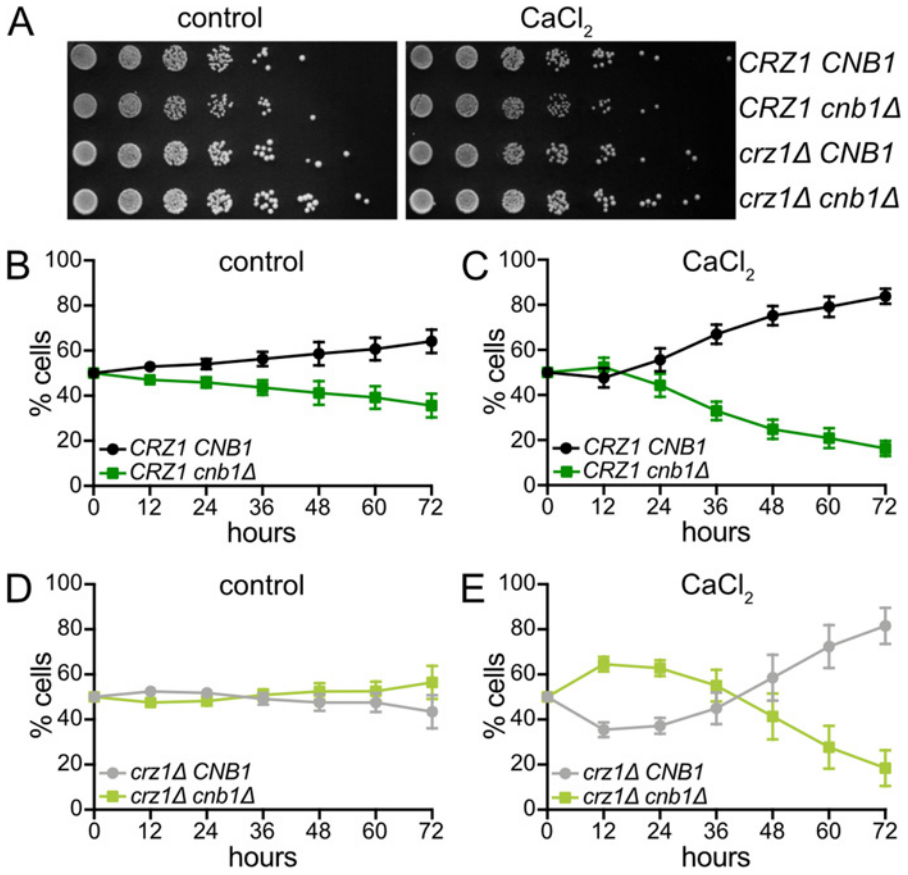

FIGURE 1: CN promotes fitness in response to chronic calcium stress. (A) Five-fold serial dilutions of the indicated strains were spotted on synthetic complete media with or without 0.2 M $CaCl_2$. Plates were imaged after 72 h of growth at 30°C. (B–C) *CRZ1 CNB1* and *CRZ1 cnb1*Δ cells were cocultured in the absence (B) or presence (C) of 0.2 M $CaCl_2$. Cocultures were sampled and diluted every 12 h, and the percentage of each strain was determined at the indicated timepoints by flow cytometry. An average of $n = 11$ biological replicates is shown. Error bars indicate SDs. (D–E) Same as (B–C) in *crz1*Δ *CNB1* and *crz1*Δ *cnb1*Δ cells. An average of $n = 9$ biological replicates is shown. Error bars indicate SDs.

on plates does not always reveal modest differences in proliferation rate, we also examined the competitive growth of CN mutant strains grown in coculture with a wild-type (WT) strain in a more sensitive assay (Conti *et al.*, 2022). Briefly, one strain expressing GFP is cocultured with a strain expressing a mutated, nonfluorescent GFP(Y66F) (Supplemental Figure S1A). This coculture is maintained in logarithmic phase by dilution at regular intervals and the opposing GFP markers allow the relative percentages of each strain to be monitored over time by flow cytometry. Importantly, we observe equivalent fitness in strains expressing both WT GFP and nonfluorescent GFP(Y66F) (Supplemental Figure S1, B and C). Using this approach, we found that deletion of *CNB1* resulted in a modest proliferative defect under optimal growth conditions consistent with CN having few defined functions in the absence of stress (Figure 1B) (Cyert, 2003; Cyert and Philpott, 2013). In contrast, there was a much stronger fitness defect in *cnb1*Δ mutant cells when cocultured with WT in the presence of $CaCl_2$, indicating that CN is required for fitness in this condition (Figure 1C).

The transcription factor Crz1 is activated by CN and regulates the expression of genes important for adaptation to $CaCl_2$ (Stathopoulos-Gerontides *et al.*, 1999; Yoshimoto *et al.*, 2002). Notably, Crz1 is known to impact fitness in response to $CaCl_2$ though the severity of Crz1-dependent growth phenotypes differs between studies (Figure 1A; Supplemental Figure S1, D and E) (Polizotto and Cyert, 2001; Mulet *et al.*, 2006; Ferreira *et al.*, 2012; Zhao *et al.*, 2013; Xu *et al.*, 2019; Hsu *et al.*, 2021). This raised the possibility that the CN-dependent fitness defect that we observed resulted from a failure to activate Crz1. If this is true, then *crz1*Δ and *crz1*Δ *cnb1*Δ cells should have equivalent fitness in the presence and absence of $CaCl_2$. Interestingly, while the *crz1*Δ and *crz1*Δ *cnb1*Δ mutants had equal fitness under optimal growth conditions, CN-dependent fitness differences were observed when these strains were cocultured in the presence of $CaCl_2$ (Figure 1, D and E). Notably, *cnb1*Δ and *crz1*Δ *cnb1*Δ cells did not display fitness defects within the first 12 h of $CaCl_2$ treatment (Figure 1, C and E), which is consistent with fact that CN promotes a transient cell cycle arrest immediately following exposure to $CaCl_2$ (Leech *et al.*, 2020). This arrest is lengthened in the absence of *CRZ1* and, accordingly, the *crz1*Δ *cnb1*Δ mutant exhibited a more pronounced growth advantage during the first 12 h of $CaCl_2$ exposure (Figure 1E). Despite these early fitness benefits, both *cnb1*Δ and *crz1*Δ *cnb1*Δ cells were depleted from the cocultures after 72 h indicating that CN maintains fitness during chronic $CaCl_2$ in both the presence and absence of Crz1 (Figure 1, C and E). However, the Crz1-dependent and Crz1-independent mechanisms by which CN promotes fitness are unknown.

Crz1 is required to inactivate CN

CN is strongly activated within minutes of exposure to $CaCl_2$ and is subsequently inactivated as cells adapt (Stathopoulos-Gerontides *et al.*, 1999; Leech *et al.*, 2020; Flynn and Benanti, 2022). However, the timing of CN inactivation and adaptation during prolonged stress exposure is unclear. To better understand the response to chronic stress, we monitored CN activity as cells grew in $CaCl_2$ for 72 h using a fluorescent reporter, CNR-C, which is a GFP-tagged, nonfunctional fragment of Crz1. CN-dependent dephosphorylation of CNR-C can be detected by Western blotting. However, because CNR-C phosphorylation status is only correlated with CN activity, we also examined CNR-C nuclear localization as an additional measure of CN activation. Consistent with previous studies (Stathopoulos-Gerontides *et al.*, 1999; Leech *et al.*, 2020; Flynn and Benanti, 2022), we observed CN-dependent changes in CNR-C within 10 min of $CaCl_2$ treatment and both WT and *crz1*Δ cells initially activated CN to similar extents, as shown by the rapid appearance of the higher mobility CNR-C species and increased nuclear signal (Figure 2, A and B; Supplemental Figure S2A). In WT cells, CN was inactivated within 3 h after $CaCl_2$ treatment as indicated by the reappearance of the phosphorylated, lower mobility CNR-C species and loss of nuclear signal (Figure 2, A and B; Supplemental Figure S2A). However, even 72 h after $CaCl_2$ exposure, CNR-C was still dephosphorylated and localized in the nucleus in 40–50% of *crz1*Δ cells (Figure 2, D and E; Supplemental Figure S2B). Treatment with FK506, but not a control buffer (ET), resulted in loss of nuclear localization and rephosphorylation of CNR-C (Supplemental Figure S3), confirming that CN remains active at these extended timepoints. These observations demonstrate that Crz1 is required to inactivate CN and are consistent with Crz1 acting in a negative feedback loop to shut off CN signaling as cells adapt to stress (Cyert, 2003).

In response to acute $CaCl_2$ stress, CN delays progression through multiple phases of the cell cycle in combination with the stress-activated MAPKs Hog1 and Mpk1 (Mizunuma *et al.*, 1998, 2001; Yokoyama *et al.*, 2006; Leech *et al.*, 2020; Flynn and Benanti, 2022). This suggested that the fitness defects of CN mutant cells (Figure 1, C and E) may be due to slowed cell cycle progression. One way that CN delays the cell cycle is by inhibiting Cdk1 activity. Activation of CN, alongside Hog1 and Mpk1, indirectly activates the kinase Swe1, which then phosphorylates Cdk1 on Y19 (Cdk1-P) to inhibit Cdk1 activity and delay cell cycle progression (Mizunuma *et al.*, 1998, 2001; Clotet *et al.*, 2006). As previously reported (Mizunuma *et al.*, 1998, 2001; Leech *et al.*, 2020), exposure to $CaCl_2$ triggered an increase in Cdk1-P and a transient cell cycle arrest (Figure 2A; Supplemental Figure S4). After 10 min of $CaCl_2$ treatment, levels of Cdk1-P were comparable in all genotypes consistent with redundant control of Cdk1 inhibition during stress (Figure 2C). However, CN was required to maintain the inhibitory phosphorylation on Cdk1 at timepoints longer than 12 h (Figure 2D). Because cells lacking Cnb1 display a proliferative defect in competitive growth assays (Figure 1, C and E), this suggests that the observed proliferation defect is not the result of increased Cdk1 inhibition. Consequently, CN must regulate additional processes to promote fitness during chronic stress.

Gene expression changes in response to chronic calcium stress

To understand the physiological changes that cells undergo in response to chronic stress, we used RNA sequencing (RNA-seq) to measure gene expression during long-term growth in $CaCl_2$ (Supplemental Figure S5A). To determine the role of CN and Crz1 in this process, we also examined gene expression in the *cnb1*Δ, *crz1*Δ, and *crz1*Δ *cnb1*Δ mutants over 72 h of $CaCl_2$ treatment. In response to $CaCl_2$, approximately half of the genome was differentially expressed at one or more timepoints and these genes were highly overlapping across genotypes (Supplemental Figure S5, B and C). This was in stark contrast to the changes that occurred in response to chronic KCl treatment, a stressor that does not require CN for fitness, in which fewer than 200 genes were differentially expressed after 48 h of treatment (Supplemental Figure S6, A–C; Supplemental Data File S1). To examine the categories of genes changing in expression over time in response to $CaCl_2$, we applied hierarchical clustering and found that, in all genotypes, differentially expressed genes fell into two broad clusters of genes whose expression mainly increased or decreased over time (Supplemental Figure S5D; Supplemental Data File S2). Gene Ontology (GO)-term enrichment analysis of upregulated and downregulated clusters in each genotype revealed several commonly regulated biological processes (Supplemental Figure S5, E–H; Supplemental Data File S2). Similar results were obtained using gene set enrichment analysis (GSEA) to identify gene sets that were significantly correlated with each the genotype (Figure 3; Supplemental Data File S3). The most notable processes that changed were related to translation/ribosome biogenesis, amino acid synthesis, ion transport, and mitochondrial function (Figure 3; Supplemental Figure S5, E–H).

One striking feature of the response to chronic $CaCl_2$ is how it differed from the well-defined ESR transcriptional program (Supplemental Figure S6D) (Gasch *et al.*, 2000; Causton *et al.*, 2001). For example, genes involved in translation and ribosome biogenesis, which are downregulated in the ESR immediately following stress, were upregulated during chronic $CaCl_2$ stress (Figure 3; Supplemental Figure S5, E–H). Interestingly, upregulation of ribosome biogenesis genes was dependent upon Crz1 but not CN, since these categories of genes were depleted in both *CNB1* and *cnb1*Δ cells lacking Crz1. Conversely, genes involved in processes related to amino acid biosynthesis and transport were significantly downregulated in a Crz1-dependent manner.

In addition to categories displaying Crz1-dependent enrichment or depletion, some processes shared common regulation across all genotypes (Figure 3; Supplemental Figure S5, E–H). For example, we observed enrichment among upregulated genes for processes related to ion transport. Many of these genes are involved in iron transport across the plasma, vacuolar, and endoplasmic reticulum membranes, indicating that regulation of iron availability may be important during adaptation to chronic $CaCl_2$ stress. Lastly, processes related to mitochondrial function including mitochondrial translation, cellular respiration, and the electron transport chain (ETC) were enriched among downregulated genes in all genotypes (Figure 3; Supplemental Figure S5, E–H). This finding highlights another way in which chronic stress differs from the ESR, since mitochondrial function is upregulated in the ESR during the acute stress response (Gasch *et al.*, 2000; Causton *et al.*, 2001).

CN and Crz1 regulate translation, mitochondrial loss, and viability during prolonged stress

Our data demonstrate that ribosome biogenesis genes are upregulated in *CRZ1* cells independent of CN (Figure 4A). We hypothesized that *CRZ1* cells may have increased translational capacity following exposure to $CaCl_2$ and should therefore be more resistant to translational inhibition. To test this, we evaluated growth in the presence of sublethal doses of the translation inhibitor

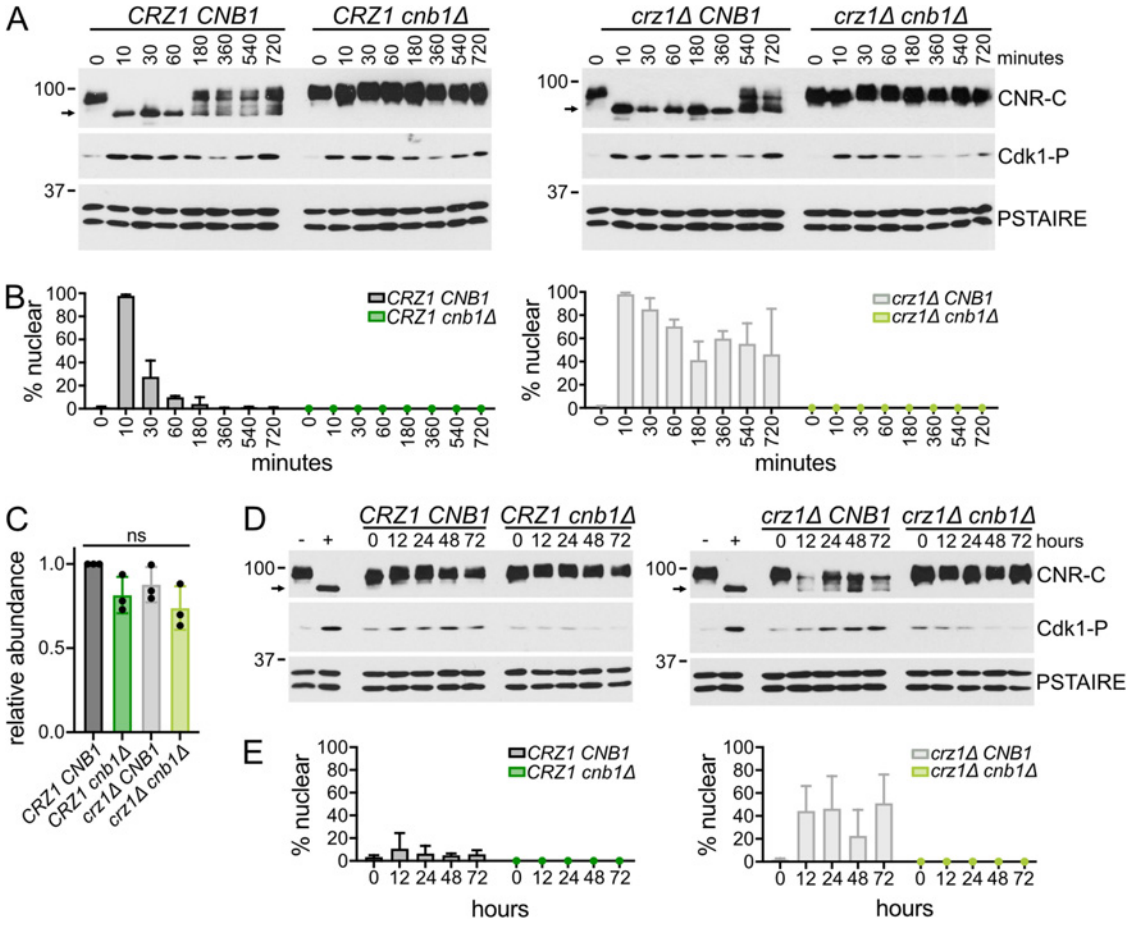

FIGURE 2: Crz1 is required to inactivate CN. (A) *CRZ1 CNB1*, *CRZ1 cnb1*Δ, *crz1*Δ *CNB1*, and *crz1*Δ *cnb1*Δ cells were grown in media with or without 0.2 M $CaCl_2$. Samples were collected at the indicated times and Western blots were performed for CNR-C ($Crz1^{14\text{-}424}$-GFP), Cdk1 phosphorylated on Y19 (Cdk1-P), and PSTAIRE (loading control). Arrows indicate dephosphorylated CNR-C. (B) Cells from A were prepared for imaging as described in the *Materials and Methods*, and the percentage of cells with nuclear CNR-C signal was calculated. An average of $n = 3$ biological replicates is shown, and error bars indicate SDs. (C) The relative abundance of Cdk1-P at t = 10 min from A was calculated by normalizing the Cdk1-P signal to PSTAIRE. The abundance of Cdk1-P in each genotype was calculated relative to Cdk1-P abundance in *CRZ1 CNB1* cells. An average of $n = 3$ experiments is shown, and error bars indicate SDs. Significance determined using a repeated measures one-way ANOVA with Geisser–Greenhouse correction and Holm–Šídák's multiple comparisons test; ns = nonsignificant. (D) *CRZ1 CNB1*, *CRZ1 cnb1*Δ, *crz1*Δ *CNB1*, and *crz1*Δ *cnb1*Δ cells were grown in media with or without 0.2 M $CaCl_2$ and diluted every 12 h. Samples were collected at the indicated times and Western blots were performed as in A. Arrows indicate dephosphorylated CNR-C. As a control for CNR-C dephosphorylation, WT cells before, "−", and after, "+",10 min of 0.2 M $CaCl_2$ treatment are shown. (E) Cells from D were prepared as in B. An average of $n = 9$ biological replicates in shown, error bars indicate SDs.

cycloheximide (CHX). Following 72 h of growth in $CaCl_2$, *CRZ1* cells were more tolerant to CHX compared with cells lacking Crz1 as well as identical strains that were not treated with $CaCl_2$ (Figure 4B). These data indicate that Crz1 increases the translational capacity of cells in response to $CaCl_2$ through a CN-independent mechanism and suggest that cells may require more ribosomes to survive and proliferate in chronic stress.

Our gene expression data also predict that mitochondrial function is reduced during chronic $CaCl_2$ exposure, since the expression of genes encoding proteins with mitochondrial functions is decreased in all genotypes (Figure 3; Supplemental Figure S5, E–H). A critical role of the mitochondria is to produce ATP via oxidative phosphorylation (Alberts *et al.*, 1994). In agreement with the GSEA and GO-term analyses, we observed $CaCl_2$-dependent downregulation of genes involved in the ETC (Figure 4C). While ETC transcripts decreased in all genotypes following the addition of $CaCl_2$, this downregulation was less severe in cells lacking Crz1. Decreased expression of ETC genes has been previously linked to the loss of functional mitochondria (Epstein *et al.*, 2001). Consistent with that study, we observed an increased proportion of petite colonies that cannot grow on nonfermentable carbon sources in all genotypes except the *crz1*Δ mutant, which maintains active CN throughout the time course (Figure 2; Figure 4D). Notably, changes in petite frequency generally correlated with the degree of ETC transcript downregulation in each genotype (Figure 4C). These data indicate that chronic $CaCl_2$ stress triggers mitochondrial dysfunction and suggest that CN activity helps prevent mitochondrial loss.

Increases in cytosolic calcium concentrations have been shown to precede mitochondrial permeabilization, which impairs mitochondrial function and triggers cell death in both yeast and mammals (Guaragnella *et al.*, 2012; Carraro and Bernardi, 2016;

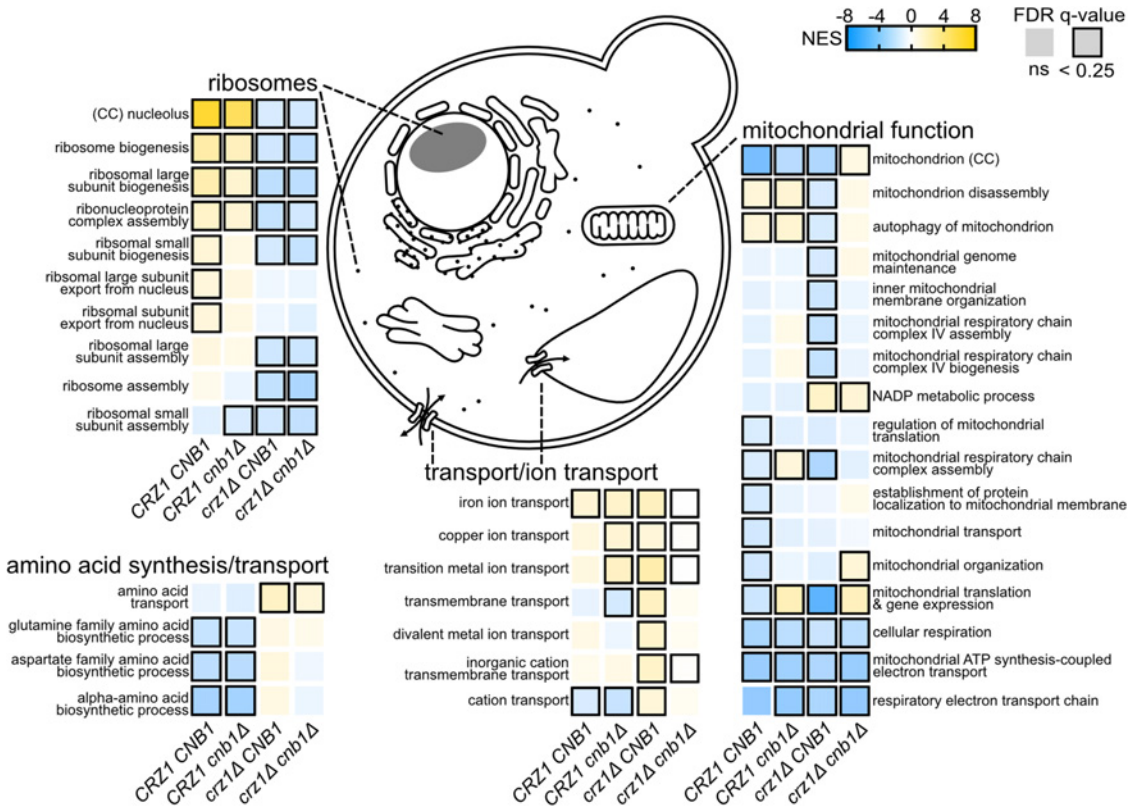

FIGURE 3: Gene expression changes in response to chronic calcium stress. GSEA of differentially expressed genes from *CRZ1 CNB1*, *CRZ1 cnb1*Δ, *crz1*Δ *CNB1*, and *crz1*Δ *cnb1*Δ strains after 72 h of growth in 0.2 M $CaCl_2$ compared with genotype-matched unstressed controls. All categories are "GO Biological Process" with the exception of those marked "CC" for "GO Cellular Component." Each square represents a genotype and colors indicate the normalized enrichment score (NES). Outlined squares indicate significantly enriched (FDR *q*-value < 0.25) categories. GSEA data for all genotypes at all timepoints are included in Supplemental Data File S3.

Frigo *et al.*, 2023). Because chronic growth in $CaCl_2$ compromises mitochondrial function (Figure 3; Figure 4, C and D), we next monitored cell viability using propidium iodide (PI) to determine whether $CaCl_2$ triggered corresponding increases in cell death (Figure 4E) (Deere *et al.*, 1998; Mirisola *et al.*, 2014; Carmona-Gutierrez *et al.*, 2018). Although CN did not impact viability in the absence of stress (Supplemental Figure S7A), we observed a significant increase in cell death in the absence of *CNB1* after 12 h in $CaCl_2$ ($p = 5.32E-04$), which steadily decreased by the 72-h timepoint, although death was still increased compared with prestress levels ($p = 2.19E-03$) (Figure 4E). This finding suggests that CN normally suppresses $CaCl_2$-induced death; however, additional mechanisms may preserve viability at later timepoints.

To examine the role of Crz1 in this process, we measured cell death in *crz1*Δ and *crz1*Δ *cnb1*Δ cells grown in the presence of $CaCl_2$. Similar to what we observed in the *cnb1*Δ single mutant, the proportion of PI-positive cells increased in the *crz1*Δ *cnb1*Δ double mutant after 12 h in $CaCl_2$ (Figure 4F; Supplemental Figure S7B), demonstrating that CN inhibits $CaCl_2$-induced death independent of Crz1 at early timepoints. However, death in the double mutant continued to increase for the remainder of the experiment (Figure 4F). This suggests that cells may be unable to adapt in the absence of Crz1, and prolonged CN activity in cells lacking Crz1 suppresses further $CaCl_2$-induced death (Figure 2). Taken together, these data suggest that both CN and Crz1 help maintain cell viability during chronic stress exposure.

CN stimulates prolonged expression of glutathione biosynthesis genes in the absence of Crz1

Prolonged exposure to $CaCl_2$ stress impairs mitochondrial function and triggers cell death in the absence of CN (Figure 4, C–F). Mitochondrial dysfunction, as well as exposure to various environmental stressors, has been shown to increase intracellular reactive oxygen species (ROS) (Brennan and Schiestl, 1996; Davidson *et al.*, 1996; Granot *et al.*, 2003; Drakulic *et al.*, 2005; Du *et al.*, 2007; Dudgeon *et al.*, 2008; Yi *et al.*, 2018; Bothammal *et al.*, 2022; Trip *et al.*, 2022). To protect against ROS-induced damage to proteins, lipids, and nucleic acids, cells rely on the antioxidant glutathione (GSH) (Jamieson, 1998). Notably, activation of CN promotes the expression of several genes required for GSH biosynthesis following acute exposure to $CaCl_2$ stress (Figure 5A; Supplemental Figure S8, A and B) (Yoshimoto *et al.*, 2002), suggesting that CN may increase GSH production to prevent mitochondrial loss and cell death.

To determine whether GSH levels are regulated in a CN-dependent manner during chronic $CaCl_2$ stress, we examined the expression of genes required to synthesize GSH (Figure 5A). In WT and *cnb1*Δ cells, there was either no change or a modest decrease in the GSH biosynthesis genes following 12 to 72 h of growth in $CaCl_2$, consistent with CN being inactive in these strains at these timepoints (Figure 2, D and E; Figure 5, B and C). In contrast, *crz1*Δ cells, in which CN remains active, maintained elevated expression of many GSH biosynthetic genes in a CN-dependent

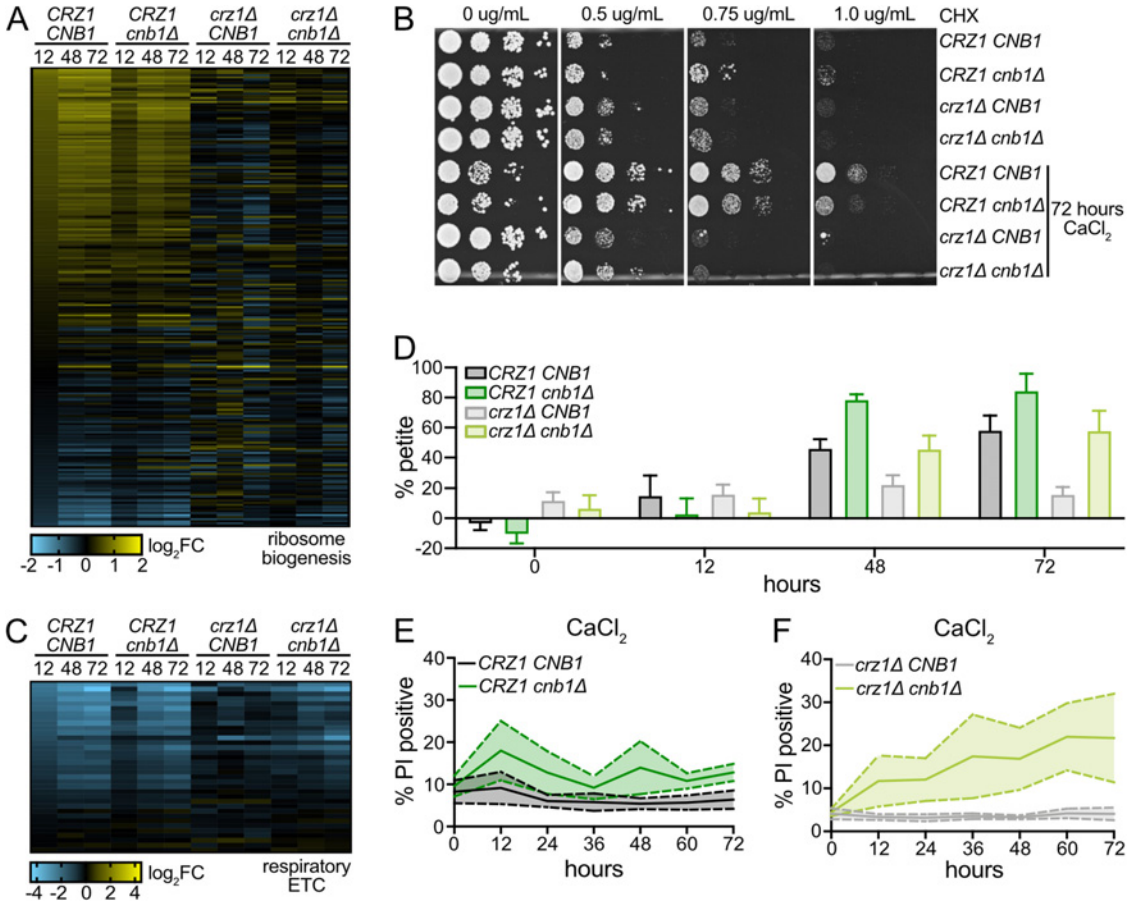

FIGURE 4: CN and Crz1 regulate translation, mitochondrial loss, and viability during prolonged stress. (A) Heatmap showing the LFC values for all genes included in "ribosome biogenesis" (GO:0042254) at the indicated timepoints compared with an unstressed control for each designated genotype. A list of genes and LFC values used to generate the heatmap are included in Supplemental Data File S4. (B) After 72 h of growth in 0.2 M $CaCl_2$, 10-fold serial dilutions of the indicated strains were spotted onto YPD agar containing the specified concentrations of CHX. Unstressed controls for each strain are included for comparison. Representative images from $n = 3$ experiments are shown. (C) As in A for all genes included in "respiratory electron transport chain" (GO:0022904). A list of genes and LFC values used to generate the heatmap are included in Supplemental Data File S4. (D) *CRZ1 CNB1*, *CRZ1 cnb1*Δ, *crz1*Δ *CNB1*, and *crz1*Δ *cnb1*Δ cells were grown for the indicated times in 0.2 M $CaCl_2$ prior to measuring petite frequency as described in the *Materials and Methods*. An average of $n = 6$ biological replicates is shown. Error bars indicate SDs. (E–F) *CRZ1 CNB1* and *CRZ1 cnb1*Δ (E) or *crz1*Δ *CNB1* and *crz1*Δ *cnb1*Δ (F) cells were grown in the presence of 0.2 M $CaCl_2$. Cultures were sampled and diluted at the indicated times and the proportion of PI-positive cells was determined by flow cytometry. Shown is an average of $n = 12$ (E) or $n = 9$ (F) biological replicates. Solid line denotes the mean and the shaded area within the dashed lines denotes the standard error of the mean. See also Supplemental Table S1.

manner (Figure 5, B and C). Interestingly, these gene expression changes are correlated with the fact that *crz1*Δ cells are protected from mitochondrial loss and downregulation of ETC genes (Figure 4, C and D; Figure 5, B and C). These findings suggest that CN promotes expression of GSH biosynthesis genes in response to $CaCl_2$, and prolonged CN activity in the absence of Crz1 maintains this pattern of gene expression.

Antioxidants rescue fitness and cell death in the absence of CN and Crz1

Having established that prolonged CN activity in the absence of Crz1 sustains the expression of GSH biosynthetic genes, we next wanted to determine whether the CN-dependent upregulation of these genes protects cells from ROS-induced death. To test this hypothesis, we first examined the competitive growth of the *crz1*Δ *cnb1*Δ strain relative to a *crz1*Δ strain, in the presence of both $CaCl_2$ and GSH (Figure 6A). Similar to what we observed in response to $CaCl_2$ alone, c*rz1*Δ *cnb1*Δ cells had a fitness benefit compared with the c*rz1*Δ mutant in the first 12 h (compare Figures 1E and 6A). However, unlike during treatment with only $CaCl_2$, the c*rz1*Δ *cnb1*Δ double mutant maintained this early proliferative advantage in the presence GSH. This result is consistent with our hypothesis that the prolonged CN activity in *crz1*Δ cells upregulates the expression of GSH biosynthetic genes to promote fitness (Figure 5, B and C; Figure 6A). In addition to rescuing the $CaCl_2$-induced fitness defect of the *crz1*Δ *cnb1*Δ mutant, GSH also reduced cell death, further supporting a GSH-dependent rescue of fitness (Figure 6B). A similar rescue of fitness and cell death was observed with homocysteine (HCys), an upstream metabolite in the GSH synthesis pathway (Figure 5A; Figure 6, C and D), suggesting that CN promotes fitness through a GSH-dependent mechanism when Crz1 is absent.

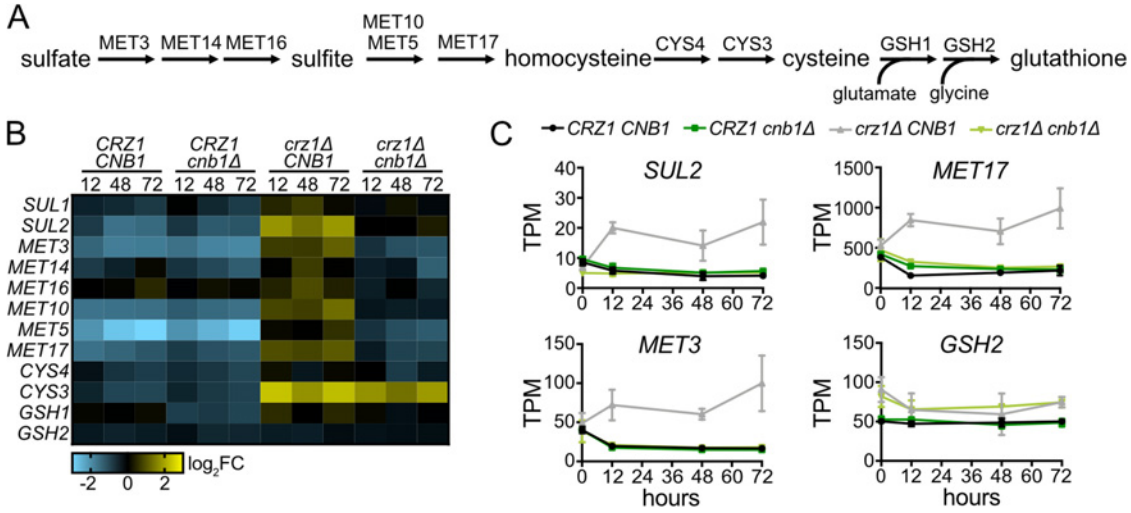

FIGURE 5: CN stimulates prolonged expression of GSH biosynthesis genes in the absence of Crz1. (A) Schematic of GSH biosynthesis in *S. cerevisiae*. (B) Heatmap showing the LFC in expression of genes involved in GSH production compared with a corresponding unstressed control in each genotype. A list of genes and LFC values used to generate the heatmap are included in Supplemental Data File S4. (C) TPM values at the indicated timepoints for *SUL2, MET3, MET17,* and *GSH2* in *CRZ1 CNB1*, *CRZ1 cnb1*Δ, *crz1*Δ *CNB1*, and *crz1*Δ *cnb1*Δ cells. An average of $n = 3$ biological replicates is shown, error bars indicate SDs.

In addition to being an antioxidant, GSH is used as a source of intracellular sulfur to produce the amino acids cysteine and methionine (Elskens *et al.*, 1991). Thus, supplementing cells with GSH or HCys could impact fitness and viability by either maintaining redox homeostasis or supporting amino acid production. To discriminate between these possibilities, we measured fitness and death in cells supplemented with the antioxidant ascorbic acid (AA), which is structurally distinct from GSH and cannot be used as a source of sulfur (Jamieson, 1998). Comparable to what we observe with GSH or HCys, AA rescued $CaCl_2$-induced fitness defects and prevented death in the *crz1*Δ *cnb1*Δ mutant (Figure 6, E and F). Together, these data demonstrate that GSH rescues fitness due to its role as an antioxidant and suggest that *crz1*Δ *cnb1*Δ cells may be dying as a result of oxidative damage.

We next examined the effect of GSH on fitness and viability in *CRZ1* cells. Because the expression of GSH synthesis genes was comparable between WT and *cnb1*Δ cells, we did not expect the fitness of *cnb1*Δ cells to be improved by the addition of GSH. As predicted, the *cnb1*Δ mutant exhibited a pronounced fitness defect in the presence of both $CaCl_2$ and GSH (Figure 6G), similar to what was observed in response to $CaCl_2$ alone (Figure 1C). Likewise, the increase in $CaCl_2$-induced cell death that occurred in *cnb1*Δ cells after 12 h did not change upon treatment with GSH (Figure 6H). These results indicate that CN promotes fitness and viability in a GSH-independent manner in cells expressing Crz1.

Altered proliferation and death differentially contribute to fitness in CN mutants

Our data suggest that CN impacts both cell cycle progression and cell death during chronic $CaCl_2$ stress (Figures 2, A and D; Figure 4, E and F; Supplemental Figure S4, A–D). However, the relative contributions of proliferation and death to CN-dependent fitness cannot be determined by measuring net population growth since it is a combination of proliferation and cell death. To determine the contributions of each, we measured the net population growth and the percentage of dead cells in monocultures growing in the presence of $CaCl_2$ (Figure 7, A–D). We then used these measurements to calculate the death rates and true proliferation rates, which excludes influences from cell death, for each strain (Schwartz *et al.*, 2020). After 12 h in $CaCl_2$, we observed a decrease in proliferation rate in all genotypes. However, while the proliferation rate mostly stabilized in cells with functional CN after 12 h, the proliferation rate of cells lacking Cnb1 continued to decrease for the remainder of the time course. We also measured an increase in the $CaCl_2$-induced death rate in the absence of *CNB1* (Figure 7, A–D), consistent with the results of the PI staining (Figure 4, E and F). These findings suggest that the CN-dependent fitness defects we observed in the coculture competitive growth assays (Figure 1, C and E) are due to both a reduced rate of cell division and an increased rate of death.

To better understand the relationship between proliferation and viability, we next used the proliferation and death rates determined from cells growing in monoculture to simulate the coculture competitive growth assays (Figure 7, E and F). Notably, this simulated growth model did not consider cell nonautonomous interactions. In doing this, we were able to recapitulate the CN-dependent fitness defects that we observed in both the presence and absence of Crz1 (Figure 1). Importantly, this finding demonstrates that our estimations of proliferation and death rates from monoculture data accurately reflect the fitness dynamics of cocultured cells. Moreover, it suggests that the effects of each genotype are cell autonomous and coculture growth is not impacted by any secreted molecules, such as GSH.

To determine whether CN affects fitness through different mechanisms in the presence and absence of Crz1, we examined the relative contributions of decreased proliferation rate and increased cell death in each genotype. To do this, we performed additional coculture simulations in which we fixed the proliferation or death rates of the competing strains (Supplemental Figure S9, A–D). We first examined fitness in the *cnb1*Δ mutant relative to WT cells. When the death rates, but not the proliferation rates, of WT and *cnb1*Δ cells were fixed the model more closely replicated the experimentally determined fitness phenotype (Supplemental Figure S9, A and B). This result indicates that a proliferative

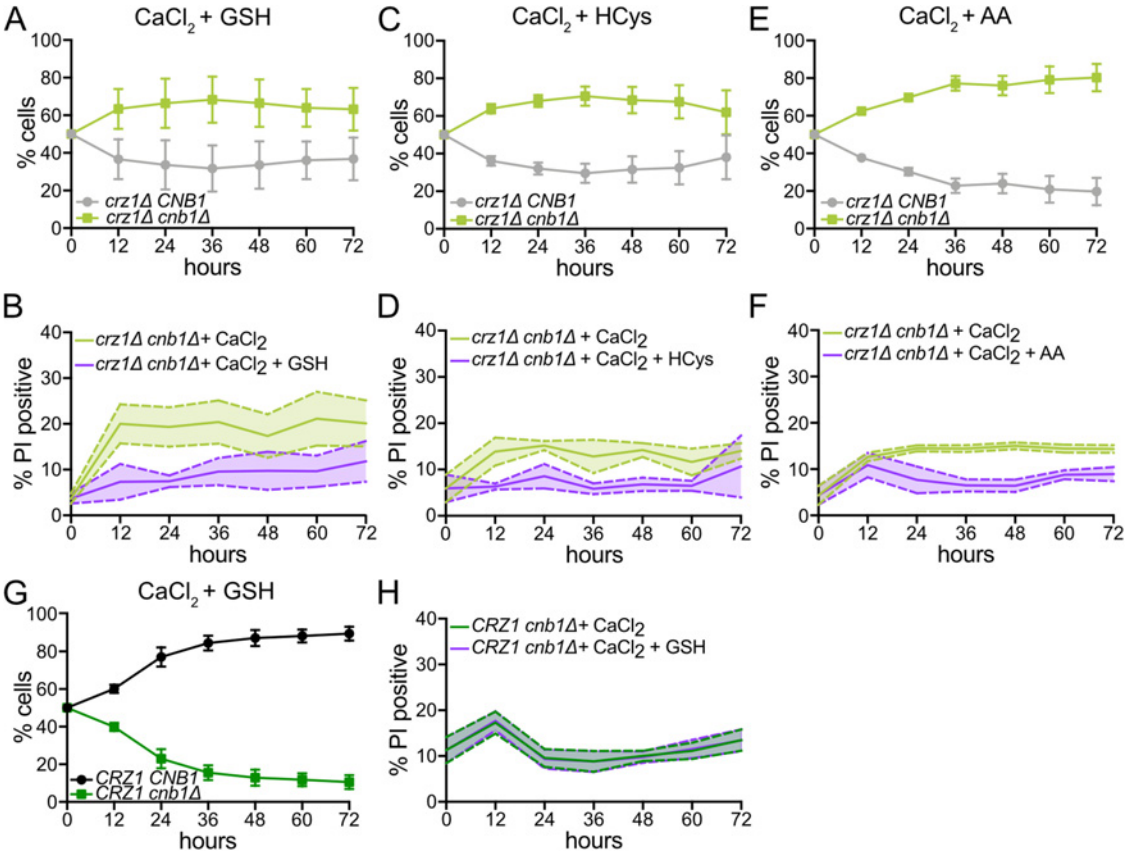

FIGURE 6: Antioxidants rescue fitness and cell death in the absence of CN and Crz1. (A) *crz1*Δ *CNB1* and *crz1*Δ *cnb1*Δ cells were cocultured in the presence of 0.2 M $CaCl_2$ and 250 μM reduced GSH. Cocultures were sampled and diluted every 12 h, and the percentage of each strain was quantified at the indicated times. An average of $n = 9$ biological replicates is shown. Error bars indicate SDs. (B) *crz1*Δ *cnb1*Δ cells were grown in the presence of 0.2 M $CaCl_2$ or 0.2 M $CaCl_2$ and 250 μM GSH and diluted every 12 h. The percentage of PI-positive cells was measured by flow cytometry. An average of $n = 9$ biological replicates is shown. Solid line denotes the mean and the shaded area within the dashed lines denotes the standard error of the mean. See also Supplemental Table S1. (C) As in A in the presence of 0.2 M $CaCl_2$ and 250 μM HCys. An average of $n = 6$ biological replicates is shown. Error bars indicate SDs. (D) As in B in the presence of 0.2 M $CaCl_2$ and 250 μM homocysteine. An average of $n = 6$ biological replicates is shown. Solid line denotes the mean and the shaded area between the dashed lines denotes the standard error of the mean. See also Supplemental Table S1. (E) As in A in presence of 0.2 M $CaCl_2$ and 5 mM AA. An average of $n = 6$ biological replicates is shown. Error bars indicate SDs. (F) As in B in the presence of 0.2 M $CaCl_2$ and 5 mM AA. An average of $n = 6$ biological replicates is shown. Solid line denotes the mean and the shaded area between the dashed lines denotes the standard error of the mean. See also Supplemental Table S1. (G) Same as A in *CRZ1 CNB1* and *CRZ1 cnb1*Δ cells. An average of $n = 9$ biological replicates is shown. Error bars indicate SDs. (H) Same as B in *CRZ1 cnb1*Δ cells. An average of $n = 12$ biological replicates is shown. Solid line denotes the mean and the shaded area within the dashed lines denotes the standard error of the mean. See also Supplemental Table S1.

defect is the primary factor decreasing fitness of the *cnb1*Δ mutant. In contrast, cell death appears to contribute more to the fitness defects in the CN mutant in the absence of Crz1 (Figure 7F; Supplemental Figure S9, C and D). When either the proliferation or death rates of the *crz1*Δ and *crz1*Δ *cnb1*Δ mutants were fixed in simulations, partial fitness defects were observed in the double mutant (Supplemental Figure S9, C and D). This suggests that fitness, while predominantly driven by decreased proliferation, is amplified by the relatively high levels of death in the absence of both CN and Crz1.

Our data demonstrate that GSH can rescue CN-dependent fitness in the absence of Crz1 (Figure 6). Therefore, we wanted to determine whether GSH rescues fitness due to effects on proliferation, viability, or both. Similar to what we observed in response to $CaCl_2$ alone, there was an initial decrease in proliferation rate in all genotypes when cells were grown in monoculture in the presence of both $CaCl_2$ and GSH (Figure 7, G–J). In the *CRZ1* background, there was a larger decrease in proliferation rate in *cnb1*Δ cells, similar to what was observed when cells were grown with $CaCl_2$ but not GSH. Consistent with the fact that GSH did not rescue fitness in cells with Crz1, the death rates in WT and *cnb1*Δ cells were largely unchanged by the addition of GSH (compare Figure 7, A and B with Figure 7, G and H). In contrast, unlike what we observe in response to $CaCl_2$ alone (Figure 7, C and D), the proliferation rate decreased to similar extents in both *crz1*Δ and *crz1*Δ *cnb1*Δ cells in the presence of $CaCl_2$ and GSH and remained constant throughout the time course (Figure 7, I and J). This suggests that GSH rescues the proliferative defect in the *crz1*Δ *cnb1*Δ mutant and is consistent with the results of the competitive growth assay (Figure 6A). Additionally, the high $CaCl_2$-induced death rate

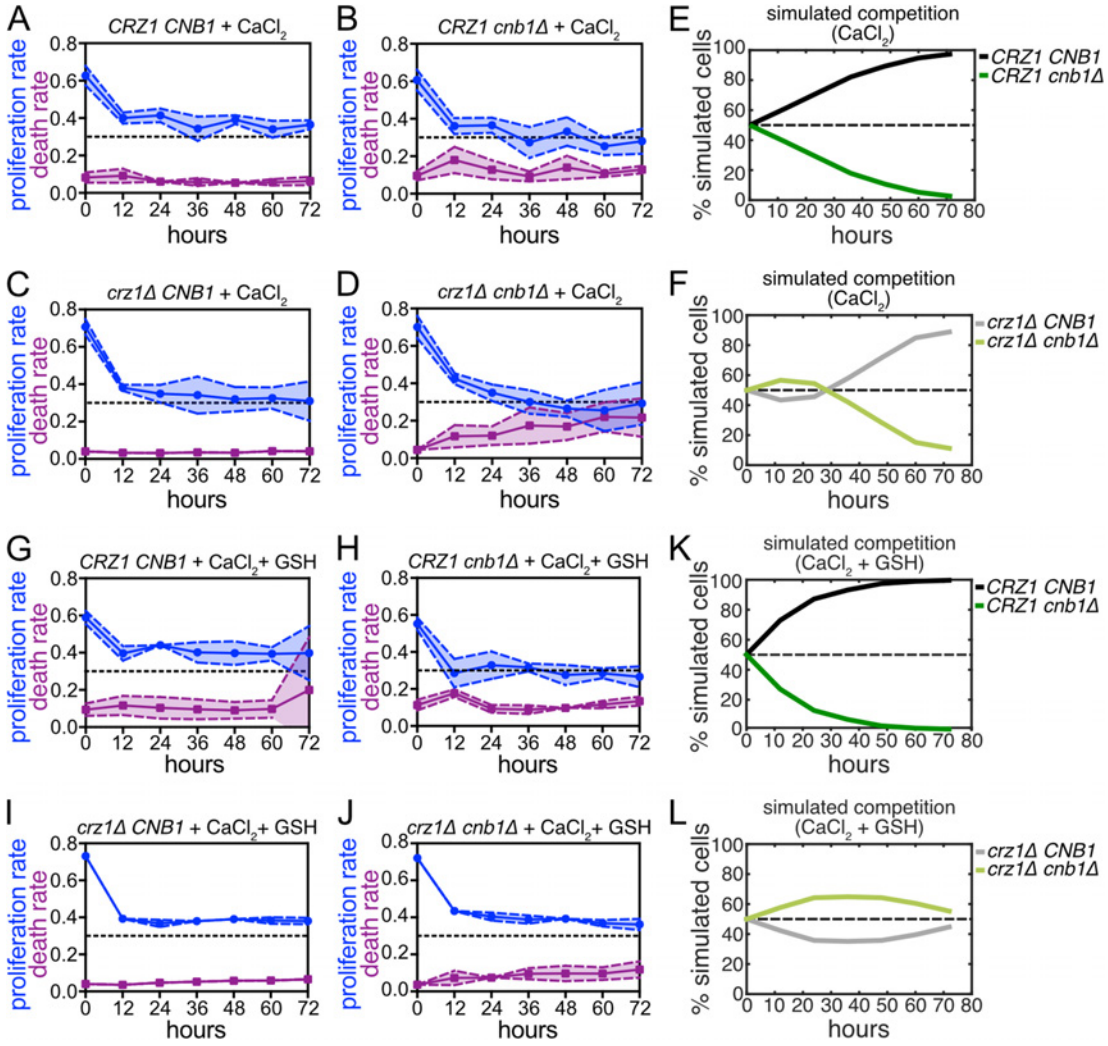

FIGURE 7: Altered proliferation and death differentially contribute to fitness in CN mutants. (A–D) Proliferation and death rates of *CRZ1 CNB1* (A), *CRZ1 cnb1*Δ (B), *crz1*Δ *CNB1* (C), and *crz1*Δ *cnb1*Δ (D) cells growing in 0.2 M $CaCl_2$ calculated from data presented in Figure 4E (A–B) and Figure 4F (C–D). (E–F) Proliferation and death rates determined in A–D were used to simulate coculture competition assays between *CRZ1 CNB1* and *CRZ1 cnb1*Δ (E) or *crz1*Δ *CNB1* and *crz1*Δ *cnb1*Δ (F) cells. (G–J) Proliferation and death rates of *CRZ1 CNB1* (G), *CRZ1 cnb1*Δ (H), *crz1*Δ *CNB1* (I), and *crz1*Δ *cnb1*Δ (J) cells growing in 0.2 M $CaCl_2$ + 250 μM GSH calculated from data presented in Supplemental Figure S8D (G), Figure 6H (H), Supplemental Figure S8E (I), and Figure 6B (J). (K–L) Proliferation and death rates determined in G–J were used to simulate coculture competition assays between *CRZ1 CNB1* and *CRZ1 cnb1*Δ (K) or *crz1*Δ *CNB1* and *crz1*Δ *cnb1*Δ (L) cells.

in the *crz1*Δ *cnb1*Δ double mutant was decreased in the presence of GSH suggesting that GSH rescues viability in addition to promoting cell cycle progression (Figure 7J).

Finally, we simulated coculture competitive growth assays in the presence of $CaCl_2$ and GSH using proliferation and death rates determined from cells grown in monoculture (Figure 7, K and L). In doing this, we accurately captured the experimentally observed fitness phenotypes of WT and *cnb1*Δ cells and confirmed that fitness differences in these strains are driven by proliferation (Figure 7K; Supplemental Figure S9, E and F). Importantly, these simulations also confirmed that GSH has no effect on fitness in the presence of Crz1. In contrast, coculture simulations of *crz1*Δ and *crz1*Δ *cnb1*Δ cells determined that GSH rescues the fitness defect of the double mutant due to effects on proliferation with modest contributions from the GSH-dependent rescue of cell death (Figure 7L; Supplemental Figure S9, G and H). Together, these data demonstrate that reduced proliferation drives the fitness defect in the absence of CN and increased cell death in cells lacking both CN and Crz1 further amplifies this fitness defect.

DISCUSSION

Coordination between proliferation and stress-defense is critical for long-term survival in challenging environments. The phosphatase CN delays cell cycle progression and promotes gene expression changes to aid adaptation immediately following exposure to $CaCl_2$ stress (Yoshimoto *et al.*, 2002). However, it was previously unknown whether CN was required for long-term survival in this condition. Here, we set out to examine the impact of CN signaling on fitness during chronic growth in $CaCl_2$. This investigation revealed that CN promotes cellular fitness by Crz1-dependent and Crz1-independent mechanisms.

CN is required to survive $CaCl_2$ exposure in opportunistic fungal pathogens, such as *Candida albicans* (Blankenship and Heitman, 2005). However, the CN-dependent fitness defect that we describe here has not been previously identified in *S. cerevisiae*. In agreement with previous studies, we did not detect a growth defect in the absence of *CNB1* when cells were grown on agar plates containing $CaCl_2$ (Figure 1A) (Nakamura *et al.*, 1996; Withee *et al.*, 1998; Mulet *et al.*, 2006; Ferreira *et al.*, 2012; Xu *et al.*, 2019). However, cells lacking Cnb1 displayed a proliferative defect in response to $CaCl_2$ when they were grown in coculture with a WT strain (Figure 1C). Notably, we did not observe any Crz1-dependent growth defects on agar plates (Figure 1A) despite previous studies reporting sensitivity or lethality in *crz1*Δ cells on agar plates containing $CaCl_2$ (Polizotto and Cyert, 2001; Mulet *et al.*, 2006; Zhao *et al.*, 2013; Xu *et al.*, 2019). Though, the loss of Crz1 did result in a competitive fitness defect in the presence of $CaCl_2$ (Supplemental Figure S1E) consistent with a previous study (Hsu *et al.*, 2021).

Our data demonstrate that CN maintains cellular fitness in $CaCl_2$ stress through both Crz1-dependent and Crz1-independent mechanisms (Figure 1). Crz1 is the best characterized downstream target of CN, and many CN-dependent functions and phenotypes are credited to the regulation of this transcription factor (Cyert, 2003; Cyert and Philpott, 2013). However, in addition to Crz1, CN directly regulates many other substrates involved diverse cellular processes including protein trafficking, membrane structure and function, cell cycle, transcription, and translation (Goldman *et al.*, 2014). Thus, it is unsurprising that CN impacts fitness in the absence of Crz1.

Although CN can maintain fitness in the absence of Crz1, our data suggest that Crz1 contributes to proper adaptation. CN remains active in cells lacking Crz1 consistent with a previous study demonstrating that Crz1 induces the expression of negative regulators of CN (Figure 2) (Yoshimoto *et al.*, 2002). These regulators include *RCN1,* which directly binds CN and inhibits phosphatase activity, and the calmodulin-dependent kinase *CMK2*, which suppresses CN signaling through an undetermined mechanism (Kingsbury and Cunningham, 2000; Xu *et al.*, 2019). Crz1 also promotes the expression of many ion channel genes, which may help restore intracellular Ca^{2+} homeostasis and shut off CN signaling (Yoshimoto *et al.*, 2002). In contrast, when Crz1 is present, most cells inactivate CN within hours of exposure to $CaCl_2$ stress suggesting that CN activity is no longer needed to survive, and cells have adapted (Figure 2). Consistent with Crz1 promoting more rapid adaptation, we observed a Crz1-dependent increase in the expression of ribosome biogenesis genes as early as 12 h after $CaCl_2$ treatment (Figures 3 and 4A). As part of the ESR, ribosome biogenesis genes are downregulated in response to stress so that transcription of stress-defense genes can increase (Gasch *et al.*, 2000; Causton *et al.*, 2001; Levy *et al.*, 2007). As adaptation occurs, these gene expression changes are reversed and translational capacity increases so that cells can resume normal growth (Levy *et al.*, 2007). We show that both WT and *cnb1*Δ cells, which express Crz1, increase the expression of ribosome biogenesis genes to enhance translational capacity and this may help cells adapt to chronic $CaCl_2$ (Figure 4, A and B). Surprisingly, although there are Crz1-dependent gene expression changes in CN mutants, we see no evidence that our CN reporter, CNR-C, is dephosphorylated or in the nucleus (Figure 2). Because CNR-C is a fragment of Crz1, it is unclear whether Crz1 is active in these cells. It is possible that there is a low level of Crz1 activation in a fraction of *cnb1*Δ cells that the reporter is not sensitive enough to detect. Alternatively, the reporter may lack an additional sequence that contributes to CN-independent Crz1 activation.

In the absence of Crz1, our data suggest that cells experience redox imbalance and ROS-induced cell death. To prevent ROS accumulation and maintain redox homeostasis cells rely on oxidant defense systems, such as GSH, which act as free radical scavengers or ROS targets (Jamieson, 1998). We found that prolonged CN activity in the absence of Crz1 promotes the upregulation of GSH biosynthesis genes, which helps cells maintain fitness and viability (Figure 5, B and C; Figure 6). CN and Crz1 are known to induce the expression of additional genes involved in the oxidative stress response (Yoshimoto *et al.*, 2002; Tsuzi *et al.*, 2004; Puigpinós *et al.*, 2014), CN may increase GSH biosynthetic gene expression through its interaction with the oxidative stress transcription factor Yap1, which contributes to the expression of GSH regulatory genes (Sugiyama *et al.*, 2000; Yokoyama *et al.*, 2006; Venters *et al.*, 2011; Goldman *et al.*, 2014). Alternatively, the transcription factor Met4, which controls the expression the *MET* genes required to produce GSH (Figure 5A), might be regulated by CN through a predicted CN-docking motif present in Met4 (Lee *et al.*, 2010; Goldman *et al.*, 2014). CN has similarly been shown to suppress cell death in response to other ROS-inducing stressors (Moser *et al.*, 1996; Huh *et al.*, 2002; Bonilla and Cunningham, 2003; Zhang *et al.*, 2006; Dudgeon *et al.*, 2008; Farrugia and Balzan, 2012; Zhao *et al.*, 2021). However, it is unclear whether CN similarly stimulates GSH production in these conditions. Finally, in mammals, CN promotes autophagy and lysosome biogenesis following activation in response to ROS-induced lysosomal Ca^{2+} release (Zhang *et al.*, 2016). These observations suggest that CN may play a conserved role in protecting cells from oxidative damage in response to diverse environmental stressors.

Cells have been shown to secrete GSH in response to environmental stressors such as heat shock and arsenite (Thorsen *et al.*, 2012; Trip and Youk, 2020). This raised the possibility that the *crz1*Δ mutant secretes GSH, in addition to upregulating GSH biosynthetic gene expression (Figure 5), which may impact the fitness of *crz1*Δ *cnb1*Δ cells when these strains are grown in coculture. To address this, we determined the proliferation rates and death rates of *crz1*Δ and *crz1*Δ *cnb1*Δ mutants growing in monoculture in the presence of $CaCl_2$ and used these rates to simulate coculture experiments (Figure 7, C, D, and F). In doing this, we were able to accurately replicate the experimentally observed coculture fitness phenotypes (compare Figure 7F and Figure 1E). These findings strongly suggest that if $CaCl_2$ does promote GSH secretion, extracellular GSH has negligible, in any, effects on the coculture fitness of *crz1*Δ and *crz1*Δ *cnb1*Δ cells.

Although the immediate response to many environmental stressors, including $CaCl_2$, has been well characterized, very little is known about the physiological changes that cells undergo to survive long-term stress exposure. Here, we have characterized the response to chronic $CaCl_2$ stress and uncovered CN-dependent mechanisms that allow cells to adapt to this environment. Our findings suggest that the requirements for adaptation change dramatically during prolonged stress exposure compared with the immediate response to stress. This is exemplified in the transcriptional differences we observe in ESR genes either immediately following $CaCl_2$ treatment or after many hours in this condition (Supplemental Figure S6D). Additionally, our data indicate that long-term adaptation is stress-specific since prolonged treatment with $CaCl_2$ and KCl elicit distinct transcriptional responses (Supplemental Figure S6, A–C). Future studies investigating long-term adaptation to

diverse conditions is needed to define the common features of the chronic ESR.

MATERIALS AND METHODS

Yeast strains and growth conditions

A complete list of strains used in this study is included in Supplemental Table S2. All strains containing deletions and/or epitope tags were generated using standard methods, as previously described (Rothstein, 1991; Longtine *et al.*, 1998). Strains were grown at 30°C in synthetic complete media (C media with 2% dextrose, 1% ammonium chloride). Where indicated, media also contained 0.2 M $CaCl_2$, 0.4 M KCl, and/or 250 μM reduced L-glutathione (Sigma), 250 μM DL-homocysteine (Sigma), or 5 mM AA (Sigma). Marker strains for competitive fitness assays (GFP+ and GFP−) were constructed as previously described (Conti *et al.*, 2022). Any additional genetic manipulations in competition strains (i.e., gene deletions) were introduced by genetic cross between the marker strains and strains containing the desired mutation. Strains in which multiple genes were deleted with the same drug resistance cassette were confirmed by PCR. All experiments were performed in biological and technical triplicate with independently derived isolates of each strain.

Serial dilution assays

Cells were grown to logarithmic phase growth in synthetic complete media. Equivalent optical densities (0.4 OD_{600}) of each sample were collected, washed, and resuspended in 1 ml of synthetic complete media. Five-fold dilutions of strains with the indicated genotypes were then plated on synthetic complete agar (C agar with 2% dextrose and 1% ammonium chloride) or synthetic complete agar containing 0.2 M $CaCl_2$ at the indicated concentrations. Plates were incubated at 30°C and imaged after 48–72 h of growth. For experiments using CHX, 10-fold serial dilutions were plated on YPD agar (2% dextrose) containing the indicated concentrations of CHX and images after 1–8 d of growth at 30°C.

Competitive fitness assays

Cocultures were generated by mixing equal proportions (1 OD_{600}) of cells expressing fluorescent GFP and nonfluorescent GFP-Y66F in 10 ml of synthetic complete media. Immediately following mixing, approximately 0.15 optical densities were collected, washed, resuspended in 2 ml of sodium citrate buffer (50 mM sodium citrate, 0.02% NaN_3, pH 7.4), and stored at 4°C for subsequent flow cytometric analysis. All cocultures were then diluted to 0.004–0.01 optical densities in 10 ml of synthetic complete media with or without stress (0.2 M $CaCl_2$ or 0.4 M KCl) and incubated at 30°C with continuous rolling. Cocultures were sampled and diluted to 0.004–0.02 optical densities, as described above, every 12 h to ensure that the population did not exceed logarithmic growth during the duration of the experiment. Following sonication, the percentage of GFP and GFP (Y66F) at each timepoint was quantified using a Guava EasyCyte HT flow cytometer and analyzed with FlowJo software. Replicates in which a fitness difference was observed between the GFP and GFP (Y66F) controls were excluded from the final analysis.

Analysis of cell cycle by flow cytometry

Approximately 0.15 ODs of cells were fixed in 70% ethanol at 4°C overnight. Following sonication, cells were treated with 0.25 mg/ml Rnase A (Biomatik) at 50°C for 1 h and 0.125 mg/ml Proteinase K (Biomatik) for an additional hour at 50°C. Following deproteination, samples were stained with 1 μM Sytox Green (Invitrogen). DNA content was measured using a Guava EasyCyte HT flow cytometer (Millipore) and analyzed with FlowJo software (FlowJo, LLC). The percentage of cells in S phase was determined from cells with a DNA content between the 1C unreplicated peak and the 2C replicated peak.

CNR-C imaging

Activation of CN was monitored using a C-terminally GFP-tagged Crz1 truncation which lacks a DNA binding domain (CNR-C). Nuclear localization following dephosphorylation of CNR-C was used as a proxy for *in vivo* CN activity. Following exposure to 0.2 M $CaCl_2$ for the indicated times, equivalent optical densities (1 OD_{600}) of cells were collected, centrifuged, and resuspended in a small volume of synthetic complete media. Where indicated, cells were treated for 15 min with 1 μg/ml FK506 (LC Laboratories) or ET buffer (90% ethanol, 10% Tween-20) to a final concentration of 0.09% ethanol and 0.01% Tween-20. Cells were imaged with equivalent exposure times on a Zeiss AxioObserver 7 microscope with a Hamamatsu Orca Fusion-BT camera and a strain lacking CNR-C was used as a control for autofluorescence. Adjustments for brightness and contrast were performed equally on all images and the percentage of cells in the population with nuclear CNR-C signal was scored by manual inspection of the images in ImageJ. A minimum of 100 cells per sample were counted at each timepoint.

Western blots

Equivalent optical densities (1 OD_{600nm}) of cells were lysed in cold TCA buffer (10 mM Tris-HCl pH 8.0, 10% trichloroacetic acid, 25 mM NH_4OAc, 1 mM Na_2EDTA) and incubated on ice. After centrifugation, pellets were resuspended in resuspension solution (0.1M Tris-HCl pH 11, 0.3% SDS) and boiled for 5 min at 95°C. Following additional centrifugation, supernatants from clarified samples were transferred to new tubes containing 4X sample buffer (250 mM Tris-HCl pH 6.8, 8% SDS, 40% glycerol, 20% β-mercaptoethanol) and boiled for 5 min at 95°C. Western blotting was performed using antibodies against GFP (clone JL8; Clontech), Y15-phosphorylated Cdk1 (anti-Phospho-cdc2, Cell Signaling Technology), and PSTAIRE (Sigma).

Multiple exposures of all Western blots were collected. Where indicated, the relative abundance of Cdk1-P was determined using ImageJ on the lightest exposure in which Cdk1-P was visible at t = 0 min. All Cdk1-P values were normalized to the loading control PSTAIRE and the abundance of Cdk1-P in each genotype after 10 min in 0.2 M $CaCl_2$ stress was calculated relative to WT.

RNA-seq and data analysis

Total RNA was purified using an acid-phenol extraction as previously described (Schmitt *et al.*, 1990) from 5 OD_{600} of cells. Poly-A enrichment, library preparation, and sequencing was performed by BGI Genomic Services. Three biological replicates of each time course were performed. All data are available in NCBI Gene Expression Omnibus (GEO) and is accessible through GEO Series accession number GSE254555.

RNA-seq analysis was performed with OneStopRNAseq (Li *et al.*, 2020). Paired-end reads were aligned to *Saccharomyces_cerevisiae*. R64-1-1, with star_2.5.3a (Dobin *et al.*, 2013), annotated with *Saccharomyces_cerevisiae*. R64-1-1.90.gtf. Aligned exon fragments with mapping quality higher than 20 were counted toward gene expression with featureCounts (Liao *et al.*, 2014). Differential expression (DE) analysis was then performed with DESeq2 (Love *et al.*, 2014). Within DE analysis "ashr" was

used to create log2 fold change (LFC) shrinkage for each comparison (Stephens, 2017). Significant DE genes were identified with the criteria FDR < 0.05. For each genotype, all genes that were significantly DE at any timepoint compared with the untreated control were classified into two groups with R package "hclust" using the complete linkage method, with 1 minus Pearson correlation as the distance. GO-term enrichment analysis on each cluster of genes in each genotype was then performed with PANTHER (Thomas *et al.*, 2022). Lists of differentially expressed genes used for GO-term analyses and the identity of genes in each cluster are included in Supplemental Data File S2. GSEA was performed with GSEA (Subramanian *et al.*, 2005) on the ranked LFC. All GSEA results are included in Supplemental Data File S3.

qRT-PCR

Reverse transcription was performed on total RNA using random primers (Promega), followed by treatment with Rnase H (New England Biolabs). Quantitative PCR was then carried out in a Lightcycler 96 thermocycler (Roche) using 2X SYBR Fast Master Mix Universal (Kapa Biosystems) and specific primers for the indicated genes (see Supplemental Table S3 for primer sequences). mRNA levels were normalized to *ACT1* to determine the relative copy number of each transcript and fold changes values were calculated by comparing the normalized expression at the indicated timepoints to the expression of the target gene prior to $CaCl_2$ addition.

Quantitation of petite frequency

Cells were grown for the indicated times in media containing 0.2 M $CaCl_2$. Serial dilutions were performed after collecting 0.1–0.2 optical densities of each culture to 1:1000. Equivalent volumes of each diluted culture were plated on YPD agar (2% dextrose) or YPG (3% glycerol) such that a few hundred colonies were formed. YPD and YPG plates were imaged after 3 and 7 d of growth at 30°C, respectively. For each genotype, petite frequency was determined from $n = 6$ biological replicates in which at least 200 colonies grew on YPD agar using the following formula:

$$\%\ petite = \left(1 - \left(\frac{\#\ colonies\ on\ YPG}{\#\ colonies\ on\ YPD}\right)\right) * 100$$

Propidium iodide staining

After sample collection and centrifugation, approximately 0.15 ODs of cells were resuspended in 2 ml sodium citrate buffer (50 mM sodium citrate, 0.02% NaN_3, pH 7.4) and stored at 4°C. Following washing with additional sodium citrate buffer, propidium iodide (PI) (MP Biomedicals, LLC) was added to each sample to a final concentration of 3 μg/ml. Samples were then incubated in the dark for 30 min prior to sonication. The percentage of PI-positive cells was quantified using a Guava EasyCyte HT flow cytometer and analyzed with FlowJo software.

Statistical analyses are included in Supplemental Table S1. To homogenize the variance and ensure robustness, the percentage of death underwent an arcsin transformation followed by a one-way analysis of variance (ANOVA) with a Randomized Complete Block Design (RCBD) to compare genotypes at the indicated timepoints. Consideration was given to control the inherent variability introduced by the blocking factor. For Figure 4E, paired *t* tests were performed between the 12-h and 0-h timepoints and the 72-h and 0-h timepoints for each genotype. All *p* values underwent Bonferroni adjustment to address the challenge of multiple inferences and ensure more stringent control over the error rate.

Antioxidant treatment

Where indicated, media was supplemented with 250 μM reduced L-glutathione (Sigma), 250 μM DL-homocysteine (Sigma), or 5 mM L-ascorbic acid (Sigma). Cultures were sampled and diluted as described above, such that cells were exposed to fresh antioxidants every 12 h. Importantly, reduced GSH was not rapidly depleted from the growth media over this 12-h interval (Supplemental Figure S8C).

To measure the concentration of GSH in growth medium over time, GSH was added to medium to a final concentration of approximately 250 μM and incubated with rolling at 30°C. Samples were then collected, and the Reduced Glutathione (GSH) Colorimetric Assay Kit (Invitrogen) was used to measure GSH concentration. Samples were prepared according to the manufacturer's instructions and a Tecan Infinite M Nano plate reader was used to measure optical densities at 405 nM.

Calculation of proliferation and death rates

For each experimental condition, doubling times of strains grown in monoculture were calculated by fitting OD_{600} values obtained at 12-h intervals to an exponential growth equation, where G = number of generations, P_0 = initial population size, and P_t = final population size:

$$2^G * P_0 = P_t \tag{1}$$

Doubling times were then determined using the following equation:

$$doubling\ time = \left(\frac{1}{\left(\frac{\#\ generations}{12\ hours}\right)}\right) * 60\ minutes \tag{2}$$

Importantly, the observed doubling time reflects the net effect, combining the true proliferation rate and true death rate. True proliferation rates and death rates were calculated using the GRADE method, as previously described (Schwartz *et al.*, 2020). Briefly, the GRADE method infers the true cell proliferation rate from a combination of 1) the experimentally measured death rate, and 2) the experimentally measured net population growth rate (GR). The average death rate was determined using flow cytometry-based measurements of percent PI positivity (described above), to determine the "fractional viability" (FV) where C_{live} = live cell number, C_{dead} = dead cell number:

$$FV = \frac{C_{live}}{C_{live} + C_{dead}} \tag{3}$$

The net population growth rate (GR value) was computed as previously described (Hafner *et al.*, 2016), using relative OD_{600} values, where C_0 = initial cell number, C_{live} = live cell number, C_{dead} = dead cell number, and C_{ctrl} = live cell number of a reference condition (defined here as a population with maximum proliferation rate and a death rate of zero):

$$GR = 2^{\left(\frac{log_2\left(\frac{C_{live}}{C_0}\right)}{log_2\left(\frac{C_{ctrl}}{C_0}\right)}\right)} - 1 \tag{4}$$

To identify the true proliferation rate and death rate, we simulated all pairwise combinations of 500 proliferation rates and 500 death rates using the following equations, where C_0 = initial cell

number, t = assay duration, τ = proliferation rate, and D_R = death rate.

$$Live\ Cell\ Number = \left(C_0 * 2^{\left(\frac{t}{\tau}\right)}\right) - \left(C_0 * 2^{\left(\frac{t}{\tau}\right)} * D_R\right) \quad (5)$$

$$Dead\ Cell\ Number = C_0 * 2^{\left(\frac{t}{\tau}\right)} * D_R \quad (6)$$

This yielded average population dynamics for 250,000 plausible proliferation rate and death rate pairs. For each simulated proliferation rate and death rate pair, the FV value and GR inhibition value (Hafner *et al.*, 2016) were calculated, as defined above. Each simulated proliferation rate and death rate pair are uniquely identifiable by their FV and GR values. Thus, the true proliferation rates and death rates of the experimental conditions were then determined by finding which simulation best matches the observed FV/GR pair.

In silico coculture experiments (Figure 7, E,F,K, and L; Supplemental Figure S9) were simulated using the experimentally determined proliferation rates and death rates from monoculture (described above) as follows. Two genotypes were seeded at equal cell numbers at time zero. We assumed there was no interaction between genotypes. Total live cell numbers for each genotype evolved according to Eq. 5, and live cell numbers, proliferation rates, and death rates were updated at each experimental time interval (every 12 h for 3 d). To separately evaluate the role of proliferation rate and death rate on in silico coculture dynamics, simulations were rerun, setting either the proliferation rates or death rates to be equal between the two genotypes.

Code availability

All codes are available upon request.

ACKNOWLEDGMENTS

We thank Tom Fazzio and members of the Benanti lab for helpful discussions and critical reading of the manuscript. This work was supported by National Institutes of Health grants R35GM136280 to J.A.B., and R01GM127559 to M.J.L.

REFERENCES

Alberts B, Bray D, Lewis J, Raff M, Roberts K, Watson JD (1994). Molecular Biology of the Cell 3rd ed., New York, NY: Garland Publishing Inc.

Blankenship JR, Heitman J (2005). Calcineurin is required for Candida albicans to survive calcium stress in serum. Infect Immun 73, 5767–5774.

Bonilla M, Cunningham KW (2003). Mitogen-activated protein kinase stimulation of Ca 2+ signaling is required for survival of endoplasmic reticulum stress in yeast. Mol Biol Cell 14, 4296–4305.

Bonny AR, Kochanowski K, Diether M, El-Samad H (2021). Stress-induced growth rate reduction restricts metabolic resource utilization to modulate osmo-adaptation time. Cell Rep 34, 108854.

Bothammal P, Prasad M, Muralitharan G, Natarajaseenivasan K (2022). Leptospiral lipopolysaccharide mediated Hog1 phosphorylation in Saccharomyces cerevisiae directs activation of autophagy. Microb Pathog 173, 105840.

Brennan RJ, Schiestl RH (1996). Cadmium is an inducer of oxidative stress in yeast. Mutat Res 356, 171–178.

Carmona-Gutierrez D, Bauer MA, Zimmermann A, Aguilera A, Austriaco N, Ayscough K, Balzan R, Bar-Nun S, Barrientos A, Belenky P, *et al.* (2018). Guidelines and recommendations on yeast cell death nomenclature. Microb Cell 5, 4–31.

Carraro M, Bernardi P (2016). Calcium and reactive oxygen species in regulation of the mitochondrial permeability transition and of programmed cell death in yeast. Cell Calcium 60, 102–107.

Causton HC, Ren B, Koh SS, Harbison CT, Kanin E, Jennings EG, Lee TI, True HL, Lander ES, Young RA (2001). Remodeling of yeast genome expression in response to environmental changes. Mol Biol Cell 12, 323–337.

Clotet J, Escoté X, Adrover MÀ, Yaakov G, Garí E, Aldea M, Nadal Ed, Posas F (2006). Phosphorylation of Hsl1 by Hog1 leads to a G2 arrest essential for cell survival at high osmolarity. EMBO J 25, 2338–2346.

Conti MM, Ghizzoni JM, Gil-Bona A, Wang W, Costanzo M, Li R, Flynn MJ, Zhu LJ, Myers CL, Boone C, *et al.* (2022). Repression of essential cell cycle genes increases cellular fitness. PLoS Genet 18, e1010349.

Cyert MS (2003). Calcineurin signaling in Saccharomyces cerevisiae: How yeast go crazy in response to stress. Biochem Biophys Res Commun 311, 1143–1150.

Cyert MS, Philpott CC (2013). Regulation of cation balance in Saccharomyces cerevisiae. Genetics 193, 677–713.

Davidson JF, Whyte B, Bissinger PH, Schiestl RH (1996). Oxidative stress is involved in heat-induced cell death in Saccharomyces cerevisiae. Proc Natl Acad Sci USA 93, 5116–5121.

Deere D, Shen J, Vesey G, Bell P, Bissinger P, Veal D (1998). Flow cytometry and cell sorting for yeast viability assessment and cell selection. Yeast 14, 147–160.

Dobin A, Davis CA, Schlesinger F, Drenkow J, Zaleski C, Jha S, Batut P, Chaisson M, Gingeras TR (2013). STAR: Ultrafast universal RNA-seq aligner. Bioinformatics 29, 15–21.

Drakulic T, Temple MD, Guido R, Jarolim S, Breitenbach M, Attfield PV, Dawes IW (2005). Involvement of oxidative stress response genes in redox homeostasis, the level of reactive oxygen species, and ageing in Saccharomyces cerevisiae. FEMS Yeast Res 5, 1215–1228.

Du L, Yu Y, Chen J, Liu Y, Xia Y, Chen Q, Liu X (2007). Arsenic induces caspase- and mitochondria-mediated apoptosis in Saccharomyces cerevisiae. FEMS Yeast Res 7, 860–865.

Dudgeon DD, Zhang N,Ositelu OO, Kim H, Cunningham KW (2008). Nonapoptotic death of Saccharomyces cerevisiae cells that is stimulated by Hsp90 and inhibited by calcineurin and Cmk2 in response to endoplasmic reticulum stresses. Eukaryot Cell 7, 2037–2051.

Elliott B, Futcher B (1993). Stress resistance of yeast cells is largely independent of cell cycle phase. Yeast 9, 33–42.

Elskens MT, Jaspers CJ, Penninckx MJ (1991). Glutathione as an endogenous sulphur source in the yeast Saccharomyces cerevisiae. Microbiology 137, 637–644.

Epstein CB, Waddle JA, Hale W, Davé V, Thornton J, Macatee TL, Garner HR, Butow RA (2001). Genome-wide responses to mitochondrial dysfunction. Mol Biol Cell 12, 297–308.

Farrugia G, Balzan R (2012). Oxidative stress and programmed cell death in yeast. Front Oncol 2, 64.

Ferreira RT, Silva ARC, Pimentel C, Batista-Nascimento L, Rodrigues-Pousada C, Menezes RA (2012). Arsenic stress elicits cytosolic Ca2+ bursts and Crz1 activation in Saccharomyces cerevisiae. Microbiology 158, 2293–2302.

Flynn MJ, Benanti JA (2022). Cip1 tunes cell cycle arrest duration upon calcineurin activation. Proc Natl Acad Sci USA 119, e2202469119.

Frigo E, Tommasin L, Lippe G, Carraro M, Bernardi P (2023). The haves and have-nots: The mitochondrial permeability transition pore across species. Cells 12, 1409.

Gasch AP, Spellman PT, Kao CM, Carmel-Harel O, Eisen MB, Storz G, Botstein D, Brown PO (2000). Genomic expression programs in the response of yeast cells to environmental changes. Mol Biol Cell 11, 4241–4257.

Goldman A, Roy J, Bodenmiller B, Wanka S, Landry CR, Aebersold R, Cyert MS (2014). The calcineurin signaling network evolves via conserved kinase-phosphatase modules that transcend substrate identity. Mol Cell 55, 422–435.

Granot D, Levine A, Dor-Hefetz E (2003). Sugar-induced apoptosis in yeast cells. FEMS Yeast Res 4, 7–13.

Guaragnella N, Ždralević M, Antonacci L, Passarella S, Marra E, Giannattasio S (2012). The role of mitochondria in yeast programmed cell death. Front Oncol 2, 70.

Hafner M, Niepel M, Chung M, Sorger PK (2016). Growth rate inhibition metrics correct for confounders in measuring sensitivity to cancer drugs. Nat Methods 13, 521–527.

Ho Y-H, Gasch AP (2015). Exploiting the yeast stress-activated signaling network to inform on stress biology and disease signaling. Curr Genet 61, 503–511.

Hogan PG, Chen L, Nardone J, Rao A (2003). Transcriptional regulation by calcium, calcineurin, and NFAT. Genes Dev 17, 2205–2232.

Hsu IS, Strome B, Lash E, Robbins N, Cowen LE, Moses AM (2021). A functionally divergent intrinsically disordered region underlying the conservation of stochastic signaling. PLoS Genet 17, e1009629.

Huh G, Damsz B, Matsumoto TK, Reddy MP, Rus AM, Ibeas JI, Narasimhan ML, Bressan RA, Hasegawa PM (2002). Salt causes ion disequilibrium-induced programmed cell death in yeast and plants. Plant J 29, 649–659.

Jamieson DJ (1998). Oxidative stress responses of the yeast Saccharomyces cerevisiae. Yeast 14, 1511–1527.

Kingsbury TJ, Cunningham KW (2000). A conserved family of calcineurin regulators. Genes Dev 14, 1595–1604.
Lee TA, Jorgensen P, Bognar AL, Peyraud C, Thomas D, Tyers M (2010). Dissection of combinatorial control by the Met4 transcriptional complex. Mol Biol Cell 21, 456–469.
Leech CM, Flynn MJ, Arsenault HE, Ou J, Liu H, Zhu LJ, Benanti JA (2020). The coordinate actions of calcineurin and Hog1 mediate the stress response through multiple nodes of the cell cycle network. PLoS Genet 16, e1008600.
Levy S, Ihmels J, Carmi M, Weinberger A, Friedlander G, Barkai N (2007). Strategy of transcription regulation in the budding yeast. PLoS One 2, e250.
Li R, Hu K, Liu H, Green MR, Zhu LJ (2020). OneStopRNAseq: A web application for comprehensive and efficient analyses of RNA-seq data. Genes 11, 1165.
Liao Y, Smyth GK, Shi W (2014). featureCounts: An efficient general purpose program for assigning sequence reads to genomic features. Bioinformatics 30, 923–930.
Liu J (1993). FK506 and ciclosporin: Molecular probes for studying intracellular signal transduction. Trends Pharmacol Sci 14, 182–188.
Longtine MS, McKenzie A, Demarini DJ, Shah NG, Wach A, Brachat A, Philippsen P, Pringle JR (1998). Additional modules for versatile and economical PCR-based gene deletion and modification in Saccharomyces cerevisiae. Yeast 14, 953–961.
López-Maury L, Marguerat S, Bähler J (2008). Tuning gene expression to changing environments: From rapid responses to evolutionary adaptation. Nat Rev Genet 9, 583–593.
Love MI, Huber W, Anders S (2014). Moderated estimation of fold change and dispersion for RNA-seq data with DESeq2. Genome Biol 15, 550.
Lu C, Brauer MJ, Botstein D (2008). Slow growth induces heat-shock resistance in normal and respiratory-deficient yeast. Mol Biol Cell 20, 891–903.
Matheos DP, Kingsbury TJ, Ahsan US, Cunningham KW (1997). Tcn1p/Crz1p, a calcineurin-dependent transcription factor that differentially regulates gene expression in Saccharomyces cerevisiae. Genes Dev 11, 3445–3458.
Medina DL, Paola SD, Peluso I, Armani A, Stefani DD, Venditti R, Montefusco S, Scotto-Rosato A, Prezioso C, Forrester A, *et al*. (2015). Lysosomal calcium signalling regulates autophagy through calcineurin and TFEB. Nat Cell Biol 17, 288–299.
Mirisola MG, Braun RJ, Petranovic D (2014). Approaches to study yeast cell aging and death. FEMS Yeast Res 14, 109–118.
Mizunuma M, Hirata D, Miyahara K, Tsuchiya E, Miyakawa T (1998). Role of calcineurin and Mpk1 in regulating the onset of mitosis in budding yeast. Nature 392, 303–306.
Mizunuma M, Hirata D, Miyaoka R, Miyakawa T (2001). GSK-3 kinase Mck1 and calcineurin coordinately mediate Hsl1 down-regulation by Ca2+ in budding yeast. EMBO J 20, 1074–1085.
Moser MJ, Geiser JR, Davis TN (1996). Ca2+-calmodulin promotes survival of pheromone-induced growth arrest by activation of calcineurin and Ca2+-calmodulin-dependent protein kinase. Mol Cell Biol 16, 4824–4831.
Mulet JM, Martin DE, Loewith R, Hall MN (2006). Mutual antagonism of target of rapamycin and calcineurin signaling. J Biol Chem 281, 33000–33007.
Nakamura T, Ohmoto T, Hirata D, Tsuchiya E, Miyakawa T (1996). Genetic evidence for the functional redundancy of the calcineurin-and Mpk1-mediated pathways in the regulation of cellular events important for growth inSaccharomyces cerevisiae. Mol Gen Genet 251, 211–219.
Polizotto RS, Cyert MS (2001). Calcineurin-dependent nuclear import of the transcription factor Crz1p requires Nmd5p. J Cell Biol 154, 951–960.
Puigpinós J, Casas C, Herrero E (2014). Altered intracellular calcium homeostasis and endoplasmic reticulum redox state in Saccharomyces cerevisiae cells lacking Grx6 glutaredoxin. Mol Biol Cell 26, 104–116.
Rothstein R (1991). Targeting, disruption, replacement, allele rescue: integrative DNA transformation in yeast. Methods Enzymol 194, 281–301.
Roy J, Cyert MS (2019). Identifying new substrates and functions for an old enzyme: Calcineurin. Cold Spring Harb Perspect Biol 12, a035436.
Schmitt ME, Brown TA, Trumpower BL (1990). A rapid and simple method for preparation of RNA from Saccharomyces cerevisiae. Nucleic Acids Res 18, 3091–3092.
Schwartz HR, Richards R, Fontana RE, Joyce AJ, Honeywell ME, Lee MJ (2020). Drug GRADE: An integrated analysis of population growth and cell death reveals drug-specific and cancer subtype-specific response profiles. Cell Rep 31, 107800.
Stathopoulos AM, Cyert MS (1997). Calcineurin acts through theCRZ1/TCN1-encoded transcription factor to regulate gene expression in yeast. Genes Dev 11, 3432–3444.
Stathopoulos-Gerontides A, Guo JJ, Cyert MS (1999). Yeast calcineurin regulates nuclear localization of the Crz1p transcription factor through dephosphorylation. Genes Dev 13, 798–803.
Stephens M (2017). False discovery rates: A new deal. Biostatistics 18, 275–294.
Subramanian A, Tamayo P, Mootha VK, Mukherjee S, Ebert BL, Gillette MA, Paulovich A, Pomeroy SL, Golub TR, Lander ES, *et al*. (2005). Gene set enrichment analysis: A knowledge-based approach for interpreting genome-wide expression profiles. Proc Natl Acad Sci USA 102, 15545–15550.
Sugiyama K, Izawa S, Inoue Y (2000). The Yap1p-dependent induction of glutathione synthesis in heat shock response of Saccharomyces cerevisiae. J Biol Chem 275, 15535–15540.
Thomas PD, Ebert D, Muruganujan A, Mushayahama T, Albou L, Mi H (2022). PANTHER: Making genome-scale phylogenetics accessible to all. Protein Sci 31, 8–22.
Thorsen M, Jacobson T, Vooijs R, Navarrete C, Bliek T, Schat H, Tamás MJ (2012). Glutathione serves an extracellular defence function to decrease arsenite accumulation and toxicity in yeast. Mol Microbiol 84, 1177–1188.
Trip DSL, Maire T, Youk H (2022). Fundamental limits to progression of cellular life in frigid environments. bioRxiv, 2022.06.10.495632.
Trip DSL, Youk H (2020). Yeasts collectively extend the limits of habitable temperatures by secreting glutathione. Nat Microbiol 5, 943–954.
Tsuzi D, Maeta K, Takatsume Y, Izawa S, Inoue Y (2004). Distinct regulatory mechanism of yeast GPX2 encoding phospholipid hydroperoxide glutathione peroxidase by oxidative stress and a calcineurin/Crz1-mediated Ca2+ signaling pathway. FEBS Lett 569, 301–306.
Vaeth M, Feske S (2018). NFAT control of immune function: New frontiers for an abiding trooper. F1000Res 7, 260.
Venters BJ, Wachi S, Mavrich TN, Andersen BE, Jena P, Sinnamon AJ, Jain P, Rolleri NS, Jiang C, Hemeryck-Walsh C, *et al*. (2011). A comprehensive genomic binding map of gene and chromatin regulatory proteins in Saccharomyces. Mol Cell 41, 480–492.
Withee JL, Mulholland J, Jeng R, Cyert MS (1997). An essential role of the yeast pheromone-induced Ca2+ signal is to activate calcineurin. Mol Biol Cell 8, 263–277.
Withee JL, Sen R, Cyert MS (1998). Ion Tolerance of Saccharomyces cerevisiae lacking the Ca2+/CaM-dependent phosphatase (calcineurin) is improved by mutations in URE2 or PMA1. Genetics 149, 865–878.
Xu H, Fang T, Yan H, Jiang L (2019). The protein kinase Cmk2 negatively regulates the calcium/calcineurin signalling pathway and expression of calcium pump genes PMR1 and PMC1 in budding yeast. Cell Commun Signal 17, 7.
Yi D-G, Hong S, Huh W-K (2018). Mitochondrial dysfunction reduces yeast replicative lifespan by elevating RAS-dependent ROS production by the ER-localized NADPH oxidase Yno1. PLoS One 13, e0198619.
Yokoyama H, Mizunuma M, Okamoto M, Yamamoto J, Hirata D, Miyakawa T (2006). Involvement of calcineurin-dependent degradation of Yap1p in Ca2+-induced G2 cell-cycle regulation in Saccharomyces cerevisiae. EMBO Rep 7, 519–524.
Yoshimoto H, Saltsman K, Gasch AP, Li HX, Ogawa N, Botstein D, Brown PO, Cyert MS (2002). Genome-wide analysis of gene expression regulated by the calcineurin/Crz1p signaling pathway in Saccharomyces cerevisiae. J Biol Chem 277, 31079–31088.
Zakrzewska A, van Eikenhorst G, Burggraaff JEC, Vis DJ, Hoefsloot H, Delneri D, Oliver SG, Brul S, Smits GJ (2011). Genome-wide analysis of yeast stress survival and tolerance acquisition to analyze the central trade-off between growth rate and cellular robustness. Mol Biol Cell 22, 4435–4446.
Zhang N-N, Dudgeon DD, Paliwal S, Levchenko A, Grote E, Cunningham KW (2006). Multiple signaling pathways regulate yeast cell death during the response to mating pheromones. Mol Biol Cell 17, 3409–3422.
Zhang X, Cheng X, Yu L, Yang J, Calvo R, Patnaik S, Hu X, Gao Q, Yang M, Lawas M, *et al*. (2016). MCOLN1 is a ROS sensor in lysosomes that regulates autophagy. Nat Commun 7, 12109.
Zhao Y, Du J, Zhao G, Jiang L (2013). Activation of calcineurin is mainly responsible for the calcium sensitivity of gene deletion mutations in the genome of budding yeast. Genomics 101, 49–56.
Zhao Y, Su R, Li S, Mao Y (2021). Mechanistic analysis of cadmium toxicity in Saccharomyces cerevisiae. FEMS Microbiol Lett 368, fnab095.